ACS APPLIED MATERIALS & INTERFACES

Research Article

www.acsami.org

3D Porous Graphene–Porous PdCu Alloy Nanoparticles–Molecularly Imprinted Poly(*para*-aminobenzoic acid) Composite for the Electrocatalytic Assay of Melamine

Lei Shang, Faqiong Zhao, and Baizhao Zeng*

Key Laboratory of Analytical Chemistry for Biology and Medicine (Ministry of Education), College of Chemistry and Molecular Sciences, Wuhan University, Wuhan 430072, Hubei Province, P. R. China

Supporting Information

ABSTRACT: In this work, a three-dimensional hybrid film with in- and out-of-plane pores was fabricated by using porous graphene as framework structure and porous PdCu alloy nanoparticles as building blocks. The porous PdCu alloy nanoparticles were prepared by chemical dealloying with acetic acid. The hierarchical pores had abundant active catalytic sites, and the material exhibited remarkable catalytic activity toward the oxidation of hydrazine. Based on this hybrid film, an electrochemical sensor of melamine was developed by further introducing melamine imprinted electro-polymer of *para*-aminobenzoic acid. Melamine was detected by differential pulse voltammetry using hydrazine as electrochemical probe. The detection signal was amplified due to the catalytic oxidation of hydrazine at this hybrid film. The linear determination range was 0.01−1 μM and the detection limit was 2 nM ($S/N = 3$). The sensor displayed high recognition capacity toward melamine and also showed good reproducibility and stability. It is promising in the determination of melamine in real samples.

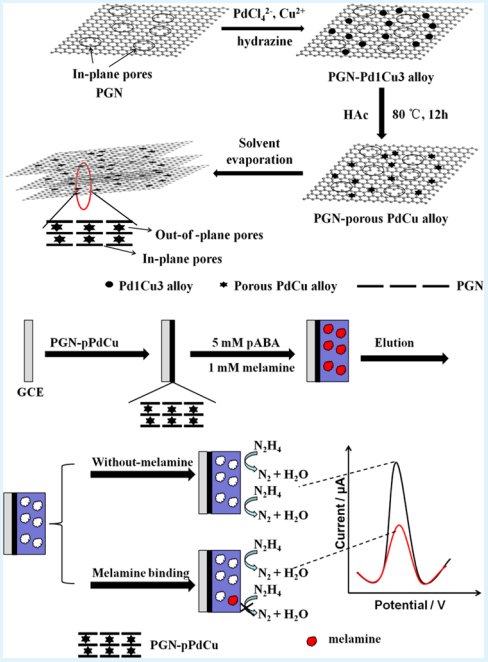

KEYWORDS: *porous graphene, porous PdCu alloy, melamine, molecularly imprinted polymer, hydrazine*

INTRODUCTION

Recently, three-dimensional (3D) graphene-based structures received extensive interest due to their exceptional electrical and mechanical properties.[1−3] For example, a 3D graphene-metal hybrid was prepared by adding noble metal nanoparticles as building blocks to isolate the graphene sheets into porous-layered structures.[3] Thus, the obtained 3D hybrid exhibited more sensitive response than individual graphene. Furthermore, the performance of 3D graphene-metal nanoparticle hybrids could be improved by tuning the structure of graphene. Currently, porous graphene (PGN) with in-plane pores has attracted extensive attention.[4−6] It was thought that porous structure might make the diffusion path length reduce and the accessible electrode−electrolyte contact area increase, so it would be better than graphene to construct 3D graphene-metal hybrids. As an example, Chen et al.[5] prepared a PGN-$NiCo_2O_4$ film as oxygen evolution reaction (OER) catalyst. It showed higher catalytic activity than graphene-$NiCo_2O_4$ film.

On the other hand, the properties of 3D graphene-metal nanoparticles hybrids can also be improved by adjusting the structure of metal nanoparticles. Porous metal structures generally have high catalysis as they have large specific surface and large number of catalytic hot spots.[7−10] Recently, Huang et al.[8] prepared a highly porous palladium nanostructure with perpendicular pore channels under mild conditions. The large specific surface and rich edge/corner atoms of the porous palladium nanostructure made it better than other reported Pd catalysts for the hydrogenation of nitrobenzene and styrene and the Suzuki coupling reaction. However, so far, 3D PGN-porous metal nanoparticles composites have not been reported, and they are expected to show higher catalytic activity than 3D graphene−metal nanoparticles composites.

Received: July 1, 2014
Accepted: October 14, 2014
Published: October 14, 2014

Melamine contains abundant amount of nitrogen (66% by mass), so it was intentionally adulterated to milk products to obtain a false increase in protein content. However, the chronic enrichment of melamine can induce renal pathology and even death, especially in babies and children.[11] So, an easy and effective method is urgently needed for the analysis of melamine in milk products. Recently, molecularly imprinted polymer (MIP)-based sensors were developed for the electrochemical detection of melamine, which showed some advantages such as predetermined selectivity, high stability, low cost, and easy preparation.[12−15] However, the sensitivities of these sensors were restricted by the limited electrochemical signals produced by poor electro-active melamine or by the mediator acting as a probe. Lately, Li et al.[16] proposed an approach to improve the sensitivity by introducing enzyme amplifier into a MIP-based melamine sensor. The detection signal was amplified because of enzyme catalytic oxidation of the H_2O_2. However, their utility was limited due to the high cost of enzyme and complex electrode fabrication.

Fortunately, sensitivity can also be improved by applying electrocatalysis of noble metals.[17−19] Zhang et al.[17] developed an electrocatalytic assay for the telomerase activity detection by using superior catalytic property of Pt nanoparticles toward hydrazine. Willner's group[19] reported an amperometric biosensor for the amplified electrochemical detection of biomolecules, based on the electrochemical reduction of H_2O_2 catalyzed by Pt nanoparticles. To date, however, there is no report about using Pd based alloy nanoparticles for the electrocatalytic assay of melamine.

In this paper, a 3D PGN-porous PdCu (pPdCu) nanoalloy structure with both in- and out-of-plane pores was prepared. The resulting hybrid displayed remarkable catalytic activity toward hydrazine oxidation. It was used for constructing an electrochemical imprinting sensor for melamine, and the sensor showed high sensitivity and selectivity.

EXPERIMENTAL SECTION

Reagents. Graphene oxide (GO) was purchased from Xianfeng Reagent Co. Ltd. (Nanjing, China). $CuSO_4{\cdot}5H_2O$, Na_2PdCl_4, hydrazine (85%), $Na_2HPO_4{\cdot}12H_2O$, $NaH_2PO_4{\cdot}2H_2O$, melamine, *para*-aminobenzoic acid (p-ABA), potassium ferricyanide, acetonitrile, and other reagents were obtained from Sinopharm Chemical Reagent Co. Ltd. (Shanghai, China). The reagents were of analytical grade and used as received.

Apparatus. Cyclic voltammetry (CV) and differential pulse voltammetry (DPV) were performed with a CHI 832c electrochemical workstation (CH Instrument Company, Shanghai, China). Electrochemical impedance spectroscopy (EIS) was obtained with a CHI 604d electrochemical workstation (CH Instrument Company, Shanghai, China). A conventional three-electrode system was applied. The working, the auxiliary, and the reference electrodes were modified glassy carbon electrode (GCE, diameter: 3 mm), platinum wire, and saturated calomel electrode (SCE), respectively. The transmission electron microscope (TEM) images were obtained using a JEM-2100 (HR) TEM (JEOL Ltd., Japan). The scanning electron microscope (SEM) images and energy dispersive X-ray spectroscopy (EDX) were obtained using a Hitachi X-650 SEM (Hitachi Co., Japan). X-ray diffraction data (XRD) was recorded with a Bruke D8 diffractometer (Germany) using Cu Kα radiation (40 kV, 40 mA) with a Ni filter.

Synthesis of Porous Graphene Oxide (PGO) and PGN. PGO was synthesized according to the report with some modification.[5] Briefly, 100 mL GO solution (0.5 mg mL^{-1}, in water) was mixed with $KMnO_4$ (500 mg) in a covered beaker for 5 h. Then, 30 mL concentrated HCl and 30 mL H_2O_2 (30%) were merged into the above solution under stirring, and they were allowed to react for 3 h. The product, that is, PGO, was washed with deionized (DI) water and then dried in an oven at 60 °C. The PGN was obtained by chemically reducing PGO using hydrazine. Specifically, PGO (100 mL, 0.1 mg mL^{-1}, in water) was mixed with hydrazine (0.04 mL), then heated to 95 °C and kept at the temperature for 12 h.

Synthesis of PGN-pPdCu Composite. The synthesis of 3D hybrid film was illustrated in Scheme 1. PGN solution (25 mL, 0.1 mg mL^{-1}) was mixed with 190 μL Na_2PdCl_4 (33 mM) and 375 μL $CuSO_4{\cdot}5H_2O$ (50 mM), and the mixture was stirred for 0.5 h. Then, 4 mL 0.1 M hydrazine was dropped into the above solution under vigorous stirring. The solution was stirred for another 0.5 h. The product, that is, PGN-Pd1Cu3 (1:3, i.e., ratio of C (Na_2PdCl_4)/C ($CuSO_4{\cdot}5H_2O$)) alloy nanoparticles hybrid, was collected by centrifugation. Then, it was mixed with acetic acid and vigorously stirred at 80 °C for 12 h. During this process, a portion of Cu dissolved from Pd1Cu3 alloy nanoparticles, resulting in the formation of porous structures. After the mixture was cooled down to room temperature, it was diluted with ethanol. The obtained product, that is, PGN-pPdCu hybrid, was washed with ethanol for at least 5 times and redispersed into 5 mL water. The PGN−solid Pd (PGN-sPd) was synthesized through the same method but in the absence of $CuSO_4{\cdot}5H_2O$.

Scheme 1. Fabrication of 3D PGN-pPdCu Hybrid Film[a]

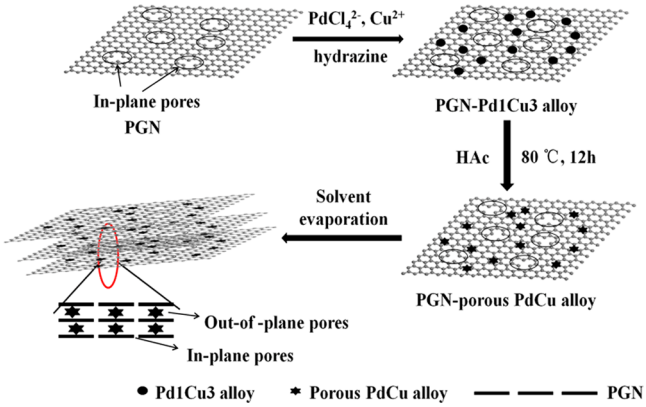

[a]PGN: porous graphene. pPdCu: porous PdCu alloy nanoparticles.

Preparation of MIP-PGN-pPdCu Modified Electrode. Prior to modification, 3 μL above-mentioned solution was dropped onto a clean GCE. After it was dried, MIP was prepared by potential cycling for 10 times between −0.6 and 1.0 V at 50 mV/s in a 0.1 M phosphate buffer solution (PBS, pH = 7.0) containing 5 mM p-ABA and 1 mM melamine, which was purged with nitrogen for 10 min before use. The obtained MIP modified electrode was denoted as MIP-PGN-pPdCu/GCE. A nonimprinted polymer modified electrode (NIP-PGN-pPdCu/GCE) was prepared by similar means but without melamine template. The MIP and NIP sensors were washed with 5 mL of extraction solvent (acetonitrile/water solution, V/V, 1:1) for three times, each for 10 min under gentle agitation. During the electrochemical detection experiment, the sensors were washed for 10 min after each measurement to remove melamine.

Voltammetric Measurements. The MIP and NIP sensors were cycled between the potential range of −0.6−0.4 V at 50 mV/s in 0.1 M PBS (pH = 7.0) to obtain a stable cyclic voltammetric curve. DPV measurement was carried out in a PBS (pH = 7.0) containing hydrazine, and the potential range was −0.6−0.4 V. Hydrazine could exhibit an oxidation peak at the MIP modified electrode. After it was immersed into a melamine solution for 5 min, the sensor displayed a decreased oxidation current for hydrazine. The determination of melamine was based on the decrease of the peak current of hydrazine. The detection process was described in Scheme 2.

Sample Pretreatment. A 5 g raw milk or milk powder sample was placed into 40 mL extraction solvent followed by sonication for 10 min. The solution was centrifuged at 4000 rpm for 10 min, and the supernatant was filtered through a 0.22 μm filter membrane. Then, the filtrate was diluted to 50 mL with extraction solvent for detection.

Scheme 2. Preparation of Electrochemical MIP Sensor and the Strategy for the Detection of Melamine

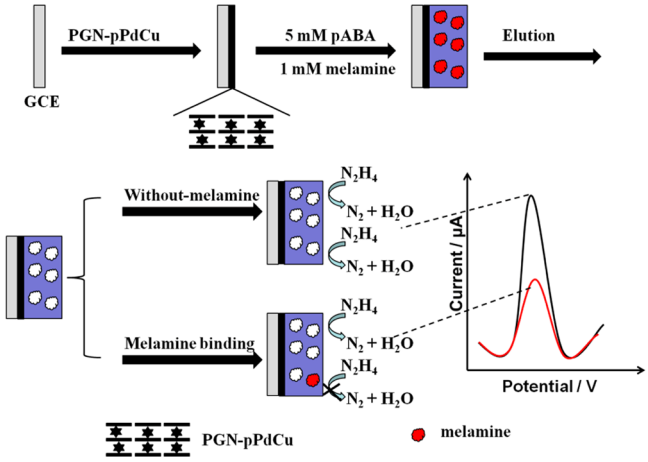

RESULTS AND DISCUSSION

Characterization of PGN-pPdCu Composite. In this paper, the PGO was obtained by oxidizing GO with $KMnO_4$, followed by etching the product MnO_2 and CO_3^{2-}/HCO_3^- with HCl and H_2O_2 (30%) to create in-plane pores on the sheet.[20] Then, the PGO was reduced to PGN by hydrazine and ammonium. As shown in Figure 1A and Supporting Information Figure S1, the PGN exhibits small in-plane pores with diameter of 10−30 nm, but graphene does not, confirming the successful preparation of PGN. To further confirm the porous structure of PGN, nitrogen adsorption−desorption isotherm was performed (Supporting Information Figure S1). The average bore diameter obtained by the Barrett−Joyner−Halenda (BJH) method was about 25 nm, which was in line with the result of TEM analysis. XRD was used to characterize the structure of PGN (Supporting Information Figure S2). There was a sharp (002) diffraction peak around $2\theta = 10°$ for PGO, corresponding to interlayer spacing of 0.85 nm.[21] After reduction, a new peak (002) at 25° appeared, meaning that the interlayer spacing of PGN sheets decreased as most oxygen-containing groups were removed. This was in line with the reported XRD results of graphene sheets.[22] However, it was reported that a certain amount of oxygen-containing functional groups of PGN could be remained after reduction by hydrazine.[5,23,24] The quantitative characterization of the remained oxygen-containing groups was performed using XPS analysis. After reduction, the percentage of sp^2 carbon of PGN increased remarkably compared with PGO (Supporting Information Figure S3), indicating that most oxygen-containing groups were removed and the conjugated graphene networks were restored after reduction. Furthermore, the peaks corresponding to C—O, C═O, and O═C—O groups, centering at 284.5, 285.6, 286.7, 287.9, and 290.3 eV respectively, still remained, making graphene sheets negatively charged (ζ-potential −41.8 mV, Supporting Information Figure S4). The electrostatic repulsion then could enable the formation of a well-dispersed black aqueous suspension.[5] In addition, there was an additional component at 285.9 eV corresponding to C bound to nitrogen, indicating that nitrogen incorporation was coupled with the reduction process.[24] Next, the Pd1Cu3 alloy nanoparticles were chemically deposited on the surface of PGN. After the metal precursors (Na_2PdCl_4 and $CuSO_4$ in molar ratio of 1:3) were added into the PGN suspension, the $PdCl_4^{2-}$ and Cu^{2+} ions were adsorbed onto the surface of PGN sheets via a coordination effect between the remained oxygen-containing groups and the $PdCl_4^{2-}$ and Cu^{2+} ions.[3] Aided by hydrazine, the ions were reduced to form PdCu

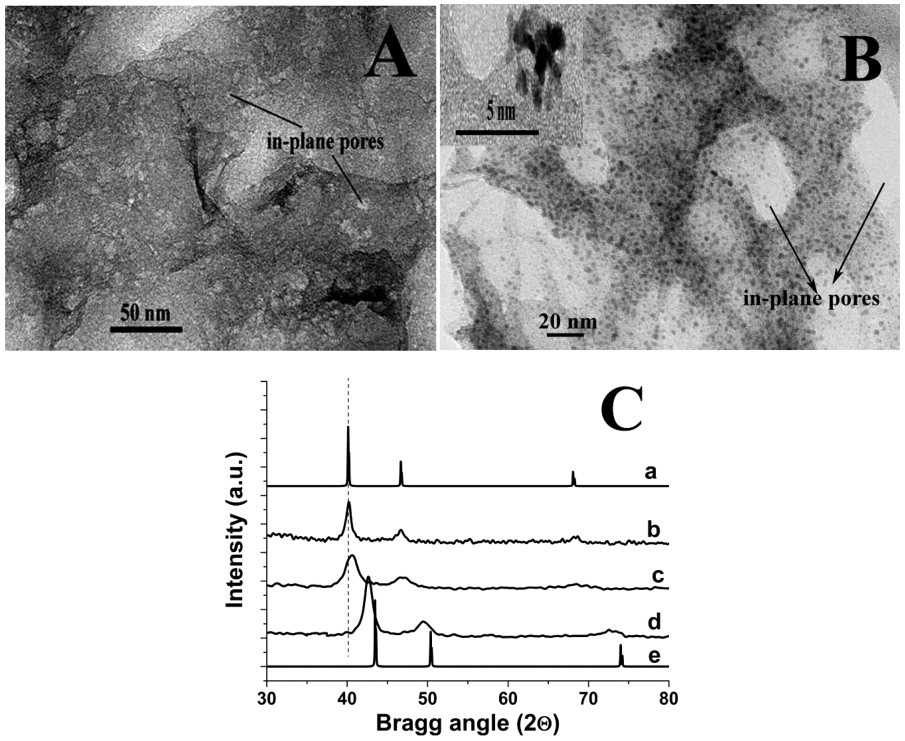

Figure 1. TEM images of PGN (A) and PGN-pPdCu (B). Inset: the magnified TEM image of pPdCu. (C) Standard XRD patterns of Pd (a) and Cu (e); XRD patterns of Pd (b), pPdCu (c), and Pd1Cu3 alloy nanoparticles (d).

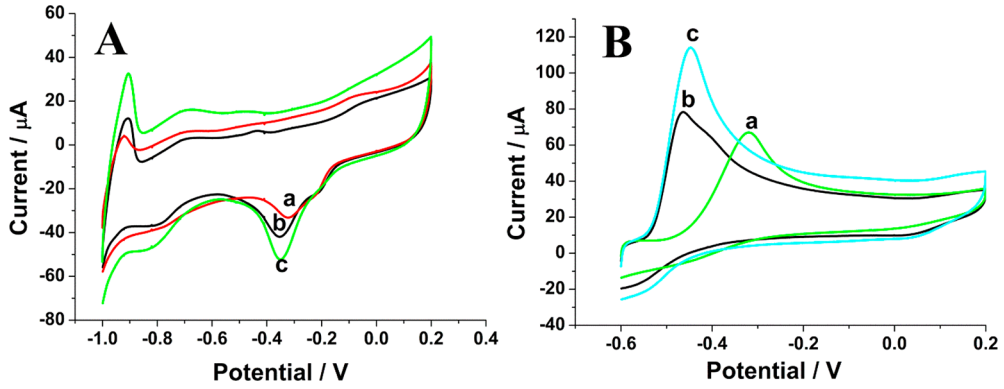

Figure 2. (A) CVs of PGN-Pd/GCE (a), GN-pPdCu/GCE (b), and PGN-pPdCu/GCE (c) in 0.5 M KOH solution. (B) CVs of PGN-Pd/GCE (a), GN-pPdCu/GCE (b), and PGN-pPdCu/GCE (c) in 0.1 M PBS (pH = 7.0) containing 3 mM hydrazine. Scan rate: 50 mV/s.

alloy nanoparticles, donated as Pd1Cu3, on the surface of PGN. The produced PGN-Pd1Cu3 hybrid could be collected by centrifugation. Subsequently, the hybrid was chemically dealloyed in order to obtain porous PdCu alloy nanoparticles. It was reported that chemical dealloying was a facile method to prepare porous Pd based alloy structures.[25−28] For example, a porous PdNi alloy nanowire was obtained by chemically dealloying in 10 wt % H_3PO_4 solution.[25] Nanoporous PdCu alloys were fabricated by selectively dealloying of Al from PdCuAl ternary alloys in 1.0 M NaOH solution.[28] In this paper, the obtained PGN-Pd1Cu3 hybrid was chemically dealloyed in acetic acid at 80 °C for 12 h. During this process, a portion of Cu dissolved from Pd1Cu3 alloy nanoparticles, resulting in the formation of porous structures. The morphology of the produced PGN-pPdCu was characterized by TEM. As can be seen in Figure 1B, the well-dispersed black dots confirmed the formation of PdCu. The magnified image (Figure 1B inset) indicated that the average diameter of the PdCu particles was about 3 nm and they were porous. Meanwhile, the dealloying process was also confirmed by EDS and XRD. The composition of Pd1Cu3 nanoparticles determined by EDS was shown in Supporting Information Figure S5. The atomic ratio of Pd/Cu was estimated to be about 1:3, which was in agreement with the concentration ratio of Na_2PdCl_4 to $CuSO_4$. After treatment with acetic acid, the ratio changed to 5.5:1. This means that most Cu dissolved, resulting in the formation of porous alloy. The structure of PdCu nanoparticles was characterized by XRD (Figure 1C). The diffraction peaks of Pd1Cu3 nanoparticles located between those of pure Pd (JCPDS 05-0681) and Cu (JCPDS 01-1241), confirming the formation of Pd1Cu3 alloy. After washing with acetic acid, the peaks of pPdCu shifted negatively compared with those of Pd1Cu3 alloy nanoparticles due to the loss of most Cu. As the Cu content was quite low in the pPdCu, its XRD pattern became very similar to that of Pd nanoparticles. Above all, these results demonstrated the formation of PGN-pPdCu hybrid. After drying in air, pPdCu served as building block to prevent graphene sheets from aggregating and isolate the graphene sheets into porous-layered structures. As can be seen in Supporting Information Figure S1, the out-of-plane pores were produced by the assembly of graphene sheets. Thus, the 3D PGN-pPdCu structure was generated, possessing both in- and out-of-plane pores.

Electrochemical Properties of Different Electrodes. The electrochemical active surface area (ECSA) is a primary parameter for evaluating the performance of electro-catalyst, and thus, it is determined here. Figure 2A presents the cyclic voltammograms (CVs) of three different modified electrodes in 0.5 M KOH solution. The peak at about −0.35 V is attributed to the reduction of PdO on the Pd surface. The ECSA of each electrode is calculated using the following equation:[29]

$$\mathrm{ECSA} = \frac{Q}{405m(\mathrm{Pd})}$$

where Q is the charge of PdO reduction (μC), m (Pd) represents the total amount of Pd (μg) on the electrode, and 405 is the charge for the reduction of a PdO monolayer in μC cm^{-2}. The calculated ECSA values are 261, 357, and 444 $m^2\ g^{-1}$ for PGN-sPd/GCE, GN-pPdCu/GCE, and PGN-pPdCu/GCE, respectively. The ECSA of PGN-pPdCu/GCE is larger than that of GN-pPdCu/GCE because the PGN can expand the Pd-electrolyte contact area. In addition, the ECSA of PGN-pPdCu/GCE is also larger than that of PGN-sPd/GCE due to the porous structure of pPdCu, which can provide more active Pd sites.

The electrocatalytic activity of the three modified electrodes was examined by taking hydrazine as model molecule. As shown in Figure 2B, compared with PGN-sPd/GCE and GN-pPdCu/GCE, PGN-pPdCu/GCE exhibits a higher peak current for hydrazine oxidation, indicating that it has higher electrocatalytic activity, arising from its larger ECSA. It is worth noting that PGN-pPdCu/GCE shows a lower peak potential than PGN-Pd/GCE. Meanwhile, the current density (normalized to ECSA) of hydrazine oxidation at PGN-pPdCu/GCE is 1.1 and 1.2 times as high as that at PGN-sPd/GCE and GN-pPdCu/GCE, respectively. The results indicate that PGN-pPdCu hybrid has higher intrinsic catalytic activity. This should be attributed to the following reasons. First, nanoporous structures, besides the effect of residual-Cu or/and the synergistic effect of alloy, lead to higher catalytic performance of PdCu alloy nanoparticles, which is in line with the previous report.[10] Second, the in-plane pores on PGN facilitates the mass transfer of reactant (hydrazine) by reducing their diffusion path length. The two factors demonstrate that porous structures of both PGN and pPdCu are favorable to the catalysis.

Electrochemical Detection of Melamine. In this paper, MIP with a so-called "gate-controlled" strategy was applied to the detection of melamine due to its high selectivity and sensitivity in the determination of poor electro-active templates.[30−32] P-ABA was chosen as the monomer because it could be easily electro-polymerized on various substrate materials and form films with good chemical and mechanical

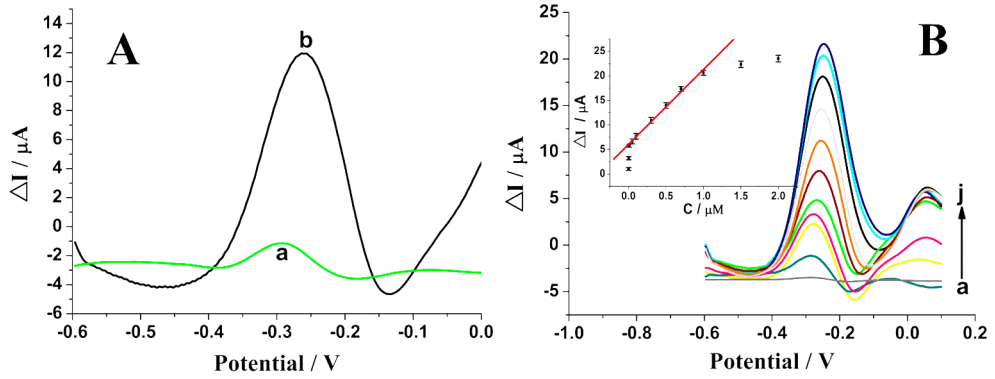

Figure 3. (A) Deduction DPVs of NIP-PGN-pPdCu/GCE (a) and MIP-PGN-pPdCu/GCE (b) between before and after rebinding of 0.5 μM melamine; (B) deduction DPVs of MIP-PGN-pPdCu/GCE between before and after rebinding melamine ((a–j) 0, 0.002, 0.01, 0.05, 0.1, 0.3, 0.5, 0.7, 1.0, 1.5, 2.0 μM). Solution for voltammetric determination: 0.1 M PBS (pH = 7.0) containing 3 mM hydrazine; pulse amplitude, 50 mV; pulse width, 0.2 s; inset, calibration curve of melamine.

stability.[33−35] Furthermore, melamine could be well imprinted in poly(p-ABA) because of the established hydrogen bonds between melamine and p-ABA.[14] As described in Scheme 2, the MIP was electro-polymerized on the surface of PGN-pPdCu; then, the template molecules were eluted in extraction solvent. Owing to the excellent catalytic activity of PGN-pPdCu hybrid toward hydrazine oxidation, hydrazine exhibited a high peak at the MIP-PGN-pPdCu/GCE. After rebinding of melamine, the peak current decreased, because the electro-inactive melamine repelled the access of hydrazine to the surface of PGN-pPdCu hybrid film. Thus, the detection signal was generated from the deduction of peak current (ΔI) of hydrazine. In order to verify the feasibility of this method, the electrochemical responses of hydrazine at PGN-pPdCu/GCE and MIP-PGN-pPdCu/GCE were recorded (Supporting Information Figure S6). Compared with PGN-pPdCu/GCE, MIP-PGN-pPdCu/GCE displayed a lower peak current and higher peak potential at about −0.2 V, indicating that the MIP film prevented hydrazine oxidation to some extent. After rebinding of melamine, the peak current further decreased and peak potential shifted positively, because the adsorbed melamine can prevent the electrochemical reaction of hydrazine at the surface of PGN-pPdCu hybrid. Thus, ΔI could be used for the determination of melamine.

Supporting Information Figure S7 presented the SEM images of PGN-pPdCu before and after the electro-polymerization of p-ABA. The PGN-pPdCu displayed the typical wrinkled sheet structure of graphene.[36] The pPdCu nanoparticles were too small (about 3 nm) to be seen in this picture. When MIP was prepared on the PGN-pPdCu, the wrinkled sheet structure was covered, and the morphology of poly(p-ABA) film occurred. This indicates the successful electro-polymerization of p-ABA on the surface of PGN-pPdCu.

EIS was also used to characterize the imprinted sensor (Supporting Information Figure S8). The EIS of PGN-pPdCu/GCE was a straight line, revealing that it had almost no electron transfer resistance (Ret). After electro-polymerization of p-ABA on the surface of PGN-pPdCu, the modified electrode displayed a much higher Ret, indicating the low conductivity of MIP film. Subsequently, when the template molecules were removed from the film, the resulting cavities allow the access of the ferricyanide and ferrocyanide ions to the electrode surface, leading to the decrease of Ret. After rebinding of melamine, the Ret became higher again because the cavities were occupied by melamine molecules.

The differential pulse voltammograms (DPVs) of melamine at MIP-PGN-pPdCu/GCE and NIP-PGN-pPdCu/GCE are presented in Figure 3A. After soaked in melamine solution, the MIP-PGN-pPdCu/GCE shows a much larger ΔI than NIP-PGN-pPdCu/GCE, indicating the higher adsorption capacity of MIP-PGN-pPdCu/GCE toward melamine. As the pH of PBS, concentration of hydrazine and rebinding time had effect on the detection of melamine, they were optimized and the results were summarized in Supporting Information Figure S9−11. Under the optimized conditions, the MIP-PGN-pPdCu/GCE was evaluated as a sensor for the quantitative determination of melamine (Figure 3B). Result shows that ΔI was linear to the melamine concentration over the range 0.01−1 μM with a regression equation of ΔI (μA) = 6.1 + 15.2 C (μM) (R = 0.9986). The detection limit was 2 nM (S/N = 3). Compared with other reported sensors,[12−14,37,38] this sensor displays a reasonable linear range and a lower detection limit (Supporting Information Table S1).

To investigate the selectivity of this electrochemical MIP sensor for melamine determination, the interference of some potential compounds in real samples was tested. The result demonstrated that 1000-fold NO_3^- and Cl^-, 500-fold glucose, lactose, SO_4^{2-}, Ca^{2+}, Mg^{2+}, and Zn^{2+}, 100-fold phenylalanine, histidine, tryptophan, and ascorbic acid, 50-fold glycine, and 10-fold cyanuric acid did not interfere with the detection of 0.5 μM melamine (i.e., signal change below 5%), indicating that the sensor had good recognition ability to melamine. This should be ascribed to the specific recognition sites formed in the polymer film. The repeatability of the sensor was investigated by seven successive detection of 0.5 μM melamine, and the relative standard deviation (RSD) of ΔI was 3.2%. To investigate the reproducibility, five modified electrodes fabricated independently by the same way were used to detect 0.5 μM melamine, and the RSD was 4.7%. After the sensor was stored in air for 3 weeks at room temperature and used for at least 25 times, it retained up to 93.5% of its original response. These results indicated that this sensor owed good repeatability, reproducibility, and stability.

To illustrate the feasibility of the MIP-PGN-pPdCu/GCE in practical analysis, raw milk and milk powder (from local supermarket) were determined by the proposed method. However, melamine was not found in both samples. Then, recovery was determined in order to check the reliability of this sensor. The results were summarized in Supporting Information Table S2 and the recovery was 93.0−102.5%. On the basis

of these data, it can be thought that this sensor is reliable and effective for the determination of melamine in real samples.

CONCLUSIONS

In conclusion, an electrochemical melamine sensor was fabricated. The sensor was constructed by 3D PGN−porous PdCu alloy hybrid film and melamine imprinted poly(p-ABA). The determination of melamine was based on the change of the anodic peak current of hydrazine, which was catalyzed by PGN-pPdCu hybrid film. The molecularly imprinted film provided high recognition ability for melamine. The resulting sensor showed high sensitivity and satisfactory selectivity and could be applied to the detection of melamine in real samples. This strategy presented here can also be used for constructing other sensors.

ASSOCIATED CONTENT

Supporting Information

TEM images of GN and PGN, SEM image of the cross-section of PGN-pPdCu film, XRD and XPS analysis of PGN, EDS of Pd1Cu3 alloy nanopariticles and pPdCu, differential pulse voltammograms to verify the feasibility of this sensor, SEM images of PGN-pPdCu/GCE and MIP-PGN-pPdCu/GCE, EIS characterization of MIP-PGN-pPdCu/GCE and two tables about comparison of different electrodes for melamine determination and measurement results of melamine in samples. This material is available free of charge via the Internet at http://pubs.acs.org.

AUTHOR INFORMATION

Corresponding Author

*Tel: 86-27-68752701. Fax: 86-27-68754067. E-mail: bzzeng@whu.edu.cn.

Notes

The authors declare no competing financial interest.

ACKNOWLEDGMENTS

The authors appreciate the financial support of the National Natural Science Foundation of China (Grant Nos.: 21075092, 21277105).

REFERENCES

(1) Stankovich, S.; Dikin, D. A.; Dommett, G. H.; Kohlhaas, K. M.; Zimney, E. J.; Stach, E. A.; Piner, R. D.; Nguyen, S. T.; Ruoff, R. S. Graphene-Based Composite Materials. *Nature* **2006**, *442*, 282−286.

(2) Wang, X.; Cao, X.; Bourgeois, L.; Guan, H.; Chen, S.; Zhong, Y.; Tang, D.-M.; Li, H.; Zhai, T.; Li, L.; Bando, Y.; Golberg, D. N-Doped Graphene-SnO_2 Sandwich Paper for High-Performance Lithium-Ion Batteries. *Adv. Funct. Mater.* **2012**, *22*, 2682−2690.

(3) Xu, P.; Yu, H.; Li, X. In Situ Growth of Noble Metal Nanoparticles on Graphene Oxide Sheets and Direct Construction of Functionalized Porous-Layered Structure on Gravimetric Microsensors for Chemical Detection. *Chem. Commun.* **2012**, *48*, 10784−10786.

(4) Zhu, Y.; Murali, S.; Stoller, M. D.; Ganesh, K. J.; Cai, W.; Ferreira, P. J.; Pirkle, A.; Wallace, R. M.; Cychosz, K. A.; Thommes, M.; Su, D.; Stach, E. A.; Ruoff, R. S. Carbon-Based Supercapacitors Produced by Activation of Graphene. *Science* **2011**, *332*, 1537−1541.

(5) Chen, S.; Qiao, S. Z. Hierarchically Porous Nitrogen-Doped Graphene−$NiCo_2O_4$ Hybrid Paper as an Advanced Electrocatalytic Water-Splitting Material. *ACS Nano* **2013**, *7*, 10190−10196.

(6) Kim, T.; Jung, G.; Yoo, S.; Suh, K. S.; Ruoff, R. S. Activated Graphene-Based Carbons as Supercapacitor Electrodes with Macro- and Mesopores. *ACS Nano* **2013**, *7*, 6899−6905.

(7) Wang, F.; Li, C.; Sun, L.-D.; Xu, C.-H.; Wang, J.; Yu, J. C.; Yan, C.-H. Porous Single-Crystalline Palladium Nanoparticles with High Catalytic Activities. *Angew. Chem., Int. Ed.* **2012**, *51*, 4872−4876.

(8) Huang, X.; Li, Y.; Chen, Y.; Zhou, E.; Xu, Y.; Zhou, H.; Duan, X.; Huang, Y. Palladium-Based Nanostructures with Highly Porous Features and Perpendicular Pore Channels as Enhanced Organic Catalysts. *Angew. Chem., Int. Ed.* **2013**, *52*, 2520−2524.

(9) Yamauchi, Y.; Tonegawa, A.; Komatsu, M.; Wang, H.; Wang, L.; Nemoto, Y.; Suzuki, N.; Kuroda, K. Electrochemical Synthesis of Mesoporous Pt−Au Binary Alloys with Tunable Compositions for Enhancement of Electrochemical Performance. *J. Am. Chem. Soc.* **2012**, *134*, 5100−5109.

(10) Park, K. H.; Lee, Y. W.; Kang, S. W.; Han, S. W. A Facile One-Pot Synthesis and Enhanced Formic Acid Oxidation of Monodisperse Pd−Cu Nanocatalysts. *Chem. − Asian J.* **2011**, *6*, 1515−1519.

(11) Guan, N.; Fan, Q.; Ding, J.; Zhao, Y.; Lu, J.; Ai, Y.; Xu, G.; Zhu, S.; Yao, C.; Jiang, L.; Miao, J.; Zhang, H.; Zhao, D.; Liu, X.; Yao, Y. Melamine-Contaminated Powdered Formula and Urolithiasis in Young Children. *N. Engl. J. Med.* **2009**, *360*, 1067−1074.

(12) Xu, G. L.; Zhang, H. L.; Zhong, M.; Zhang, T. T.; Lu, X. J.; Kan, X. W. Imprinted Sol-Gel Electrochemical Sensor for Melamine Direct Recognition and Detection. *J. Electroanal. Chem.* **2014**, *713*, 112−118.

(13) Wu, B. W.; Wang, Z. H.; Zhao, D. X.; Lu, X. Q. A Novel Molecularly Imprinted Impedimetric Sensor for Melamine Determination. *Talanta* **2012**, *101*, 374−381.

(14) Liu, Y. T.; Deng, J.; Xiao, X. L.; Ding, L.; Yuan, Y. L.; Li, H.; Li, X. T.; Yan, X. N.; Wang, L. L. Electrochemical Sensor Based on a Poly(*para*-aminobenzoic acid) Film Modified Glassy Carbon Electrode for the Determination of Melamine in Milk. *Electrochim. Acta* **2011**, *56*, 4595−4602.

(15) Khlifi, A.; Gam-Derouich, S.; Jouini, M.; Kalfat, R.; Chehimi, M. M. Melamine-Imprinted Polymer Grafts through Surface Photopolymerization Initiated by Aryl Layers from Diazonium Salts. *Food Control* **2013**, *31*, 379−386.

(16) Li, J. P.; Chen, Z. Q.; Li, Y. P. A Strategy for Constructing Sensitive and Renewable Molecularly Imprinted Electrochemical Sensors for Melamine Detection. *Anal. Chim. Acta* **2011**, *706*, 255−260.

(17) Zhang, Z.; Wu, L.; Wang, J.; Ren, J.; Qu, X. A Pt-Nanoparticle Electrocatalytic Assay Used for PCR-Free Sensitive Telomerase Detection. *Chem. Commun.* **2013**, *49*, 9986−9988.

(18) Zhai, D.; Liu, B.; Shi, Y.; Pan, L.; Wang, Y.; Li, W.; Zhang, R.; Yu, G. Highly Sensitive Glucose Sensor Based on Pt Nanoparticle/Polyaniline Hydrogel Heterostructures. *ACS Nano* **2013**, *7*, 3540−3546.

(19) Polsky, R.; Gill, R.; Kaganovsky, L.; Willner, I. Nucleic Acid-Functionalized Pt Nanoparticles: Catalytic Labels for the Amplified Electrochemical Detection of Biomolecules. *Anal. Chem.* **2006**, *78*, 2268−2271.

(20) Chen, S.; Duan, J.; Jaroniec, M.; Qiao, S. Z. Hierarchically Porous Graphene-Based Hybrid Electrodes with Excellent Electrochemical Performance. *J. Mater. Chem. A* **2013**, *1*, 9409−9413.

(21) Jeong, H. K.; Lee, Y. P.; Lahaye, R. J. W. E.; Park, M. H.; An, K. H.; Kim, I. J.; Yang, C. W.; Park, C. Y.; Ruoff, R. S.; Lee, Y. H. Evidence of Graphitic AB Stacking Order of Graphite Oxides. *J. Am. Chem. Soc.* **2008**, *130*, 1362−1366.

(22) Guo, H. L.; Wang, X. F.; Qian, Q. Y.; Wang, F. B.; Xia, X. H. A Green Approach to the Synthesis of Graphene Nanosheets. *ACS Nano* **2009**, *3*, 2653−2659.

(23) Li, D.; Muller, M. B.; Gilje, S.; Kaner, R. B.; Wallace, G. G. Processable Aqueous Dispersions of Graphene Nanosheets. *Nat. Nanotechnol.* **2008**, *3*, 101−105.

(24) Stankovich, S.; Dikin, D. A.; Piner, R. D.; Kohlhaas, K. A.; Kleinhammes, A.; Jia, Y.; Wu, Y.; Nguyen, S. T.; Ruoff, R. S. Synthesis of Graphene-Based Nanosheets via Chemical Reduction of Exfoliated Graphite Oxide. *Carbon* **2007**, *45*, 1558−1565.

(25) Du, C. Y.; Chen, M.; Wang, W. G.; Yin, G. P. Nanoporous PdNi Alloy Nanowires as Highly Active Catalysts for the Electro-Oxidation of Formic Acid. *ACS Appl. Mater. Interfaces* **2011**, *3*, 105−109.

(26) Zhang, Z. H.; Zhang, C.; Sun, J. Z.; Kou, T. Y.; Zhao, C. C. Ultrafine Nanoporous Cu−Pd Alloys with Superior Catalytic Activities towards Electro-Oxidation of Methanol and Ethanol in Alkaline Media. *RSC Adv.* **2012**, *2*, 11820−11828.
(27) Wang, W.; Ji, S.; Wang, H.; Wang, R. Nanoporous PdNi/C Electrocatalyst Prepared by Dealloying High-Ni-content PdNi Alloy for Formic Acid Oxidation. *Fuel Cells* **2012**, *12*, 1129−1133.
(28) Xu, C. X.; Liu, Y. Q.; Wang, J. P.; Geng, H. R.; Qiu, H. J. Nanoporous PdCu Alloy for Formic Acid Electro-Oxidation. *J. Power Sources* **2012**, *199*, 124−131.
(29) Shih, Z. Y.; Wang, C. W.; Xu, G.; Chang, H. T. Porous Palladium Copper Nanoparticles for the Electrocatalytic Oxidation of Methanol in Direct Methanol Fuel Cells. *J. Mater. Chem. A* **2013**, *1*, 4773−4778.
(30) Li, X.; Zhang, L.; Wei, X.; Li, J. A Sensitive and Renewable Chlortoluron Molecularly Imprinted Polymer Sensor Based on the Gate-Controlled Catalytic Electrooxidation of H_2O_2 on Magnetic Nano-NiO. *Electroanalysis* **2013**, *25*, 1286−1293.
(31) Sekine, S.; Watanabe, Y.; Yoshimi, Y.; Hattori, K.; Sakai, K. Influence of Solvents on Chiral Discriminative Gate Effect of Molecularly Imprinted Poly(ethylene glycol dimethacrylate-co-meth-acrylic acid). *Sens. Actuators, B* **2007**, *127*, 512−517.
(32) Li, X.; Li, J. P.; Yin, W. L.; Zhang, L. M. Clopyralid Detection by Using a Molecularly Imprinted Electrochemical Luminescence Sensor Based on the "Gate-Controlled" Effect. *J. Solid State Electrochem.* **2014**, *18*, 1815−1822.
(33) Zhang, Y.; Wang, J.; Xu, M. A Sensitive DNA Biosensor Fabricated with Gold Nanoparticles/Poly(*p*-aminobenzoic acid)/Carbon Nanotubes Modified Electrode. *Colloids Surf., B* **2010**, *75*, 179−185.
(34) Huang, K. J.; Xu, C. X.; Xie, W. Z.; Wang, W. Electrochemical Behavior and Voltammetric Determination of Tryptophan Based on 4-Aminobenzoic Acid Polymer Film Modified Glassy Carbon Electrode. *Colloids Surf., B* **2009**, *74*, 167−171.
(35) Benyoucef, A.; Huerta, F.; Vázquez, J. L.; Morallon, E. Synthesis and In Situ FTIRS Characterization of Conducting Polymers Obtained From Aminobenzoic Acid Isomers at Platinum Electrodes. *Eur. Polym. J.* **2005**, *41*, 843−852.
(36) Chen, L.; Tang, Y.; Wang, K.; Liu, C.; Luo, S. Direct Electrodeposition of Reduced Graphene Oxide on Glassy Carbon Electrode and Its Electrochemical Application. *Electrochem. Commun.* **2011**, *13*, 133−137.
(37) The Huy, B.; Seo, M. H.; Zhang, X.; Lee, Y. I. Selective Optosensing of Clenbuterol and Melamine Using Molecularly Imprinted Polymer-Capped CdTe Quantum Dots. *Biosens. Bioelectron.* **2014**, *57*, 310−316.
(38) Liang, R.; Zhang, R.; Qin, W. Potentiometric Sensor Based on Molecularly Imprinted Polymer for Determination of Melamine in Milk. *Sens. Actuators, B* **2009**, *141*, 544−550.